ISBN: 978-3-95450-227-1 ISSN: 2673-5490 doi:10.18429/JACoW-IPAC2022-THPOPT058

STATUS AND POWERING TEST RESULTS OF HTS UNDULATOR COILS AT 77 K FOR COMPACT FEL DESIGNS*

S. C. Richter†, [1], A. Ballarino, T. H. Nes, D. Schoerling, CERN, Geneva, Switzerland
A. Bernhard, A.-S. Müller, Karlsruhe Institute of Technology (KIT), Karlsruhe, Germany
[1]also at Karlsruhe Institute of Technology (KIT), Karlsruhe, Germany

Abstract

The production of low emittance positron beams for future linear and circular lepton colliders, like CLIC or FCC-ee, requires high-field damping wigglers. Just as compact free-electron lasers (FELs) require high-field but as well short-period undulators to emit high energetic, coherent photons. Using high-temperature superconductors (HTS) in the form of coated ReBCO tape superconductors allows higher magnetic field amplitudes at 4 K and larger operating margins as compared to low-temperature superconductors, like Nb-Ti.

This contribution discusses the development work on superconducting vertical racetrack (VR) undulator coils, wound from coated ReBCO tape superconductors. The presented VR coils were modularly designed with a period length of 13 mm. Powering tests in liquid nitrogen of multiple vertical racetrack coils were performed at CERN. The results from the measurements are presented for three VR coils and compared with electromagnetic simulations.

INTRODUCTION

Undulator magnets play a major role in accomplishing the next generation of compact and highly brilliant light sources, as they are used in synchrotrons and free-electron lasers as the main photon source with energies up to hard x-rays. When making the facilities more compact, short periods and high field undulators are crucial for delivering the needed high energetic photons for lower beam energies.

To achieve higher magnetic flux densities on the beam axis, the low-temperature superconductor (LTS) Nb-Ti was used to replace permanent magnets. An improvement of the resulting brilliance of high energy x-rays made it the state-of-the-art technology for superconducting undulators, e.g. Nb-Ti undulators operate successfully in KARA at KIT and at Argonne National Laboratory [1-3], whereas permanent magnet wigglers are used to lower the beam emittance, e.g. in PETRA III at DESY [4]. The CLIC wiggler design (3 T, 12 mm gap, 50 mm period) benefits from LTS as demonstrated with a Nb-Ti prototype at KARA, KIT [5]. An HTS version might be able to deliver around 4 T peak fields [6].

Consequently, employing high-temperature superconductors (HTS) like ReBCO (rare-earth barium copper oxide), to superconducting undulators is an attractive choice for the next upgrade. First, operations with larger temperature margins or at higher temperatures than 4 K would relax cryogenic requirements, thus reducing costs compared to LTS technologies. Second, a significant enhancement of the parameter space in terms of B_0, λ_u and gap could be shown in previous studies due to the ReBCO's high B_{c2} field at low temperatures (e.g., YBCO: $B_{c2,\perp}(4.2\,\mathrm{K}) \approx 100\,\mathrm{T}$) [7-9].

Other studies have already shown that ReBCO may be feasible for HTS undulator coils with $\lambda_u = 16$ mm to reach high current densities in the order of 2 kA/mm^2 at 4.2 K [10]. Yet, undulator periods smaller than 15 mm and quench protection stay challenging for these high currents. With our dry-wound, non-insulated (NI) design, we always give the current the option to circumvent normal conducting zones.

This paper presents and discusses the latest powering test results at 77 K of our three HTS VR undulator coils and briefly compares them to electromagnetic simulations, performed with Opera and J_c fits done at CERN [11-13].

EXPERIMENTAL SETUP

CERN and KIT are both contributing to the EU-financed CompactLight (XLS) study that explores feasibilities for a compact FEL, hence high on-axis fields for a given λ_u of 13 mm are part of the investigations [14]. Consequently, we decided to adopt this value to our modular coil design. All three presented VR undulator coils were wound with a 4 mm wide coated ReBCO tape superconductor onto a D-shaped copper winding body with an iron core (see Fig. 1). For VR coils #1 and #2, we used tape from Bruker HTS with a total thickness of 100 µm, including a 50 µm substrate and a total copper stabilizer thickness of 45 µm. For VR coil #3, 45 µm thick tape from SuperPower Inc. with a 30 µm substrate and a total copper stabilizer of 10 µm was used.

Each VR coil represents one period and thus consists of two sub-coils and two iron poles. The voltage was monitored via voltage taps on the inner- and outermost turn of each sub-coil. Two Hall probes were placed in a fixed position at a distance $d = 3.5$ mm from the iron pole face as displayed in Fig. 2. More design-related aspects can be found in Table 1. The complete design and manufacturing process were already described in previous work [15].

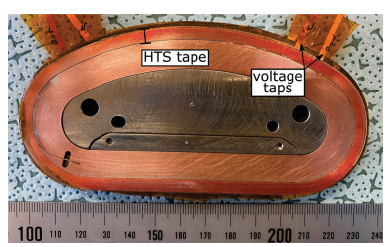

Figure 1: VR coil #3 with its four voltage taps. Scale in mm.

* This work has been supported by the Wolfgang Gentner Program of the German Federal Ministry of Education and Research.
† sebastian.richter@cern.ch

ISBN: 978-3-95450-227-1 ISSN: 2673-5490 doi:10.18429/JACoW-IPAC2022-THPOPT058

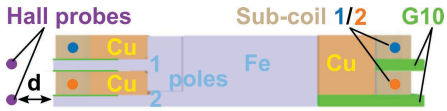

Figure 2: Cross-section of our VR coil design with the copper winding body, iron core and poles, sub-coil 1 and 2.

Table 1: Design Parameters of the VR Undulator Coils

λ_u = 13 mm	**VR coil #1,#2**	**VR coil #3**
Sub-coil x-section	4 mm × 5 mm	4 mm × 4.6 mm
HTS conductor	Bruker HTS	SuperPower
with dimensions	4 mm × 100 µm	4 mm × 45 µm
Number of turns	51	102
$J_{e,sim}$(0.6 T, 77 K)	75 A/mm^2	222 A/mm^2
$I_{c,sim}$(0.6 T, 77 K)	30 A	40 A
$B_0(I_{c,sim}, 3.5\,mm)$	0.14 T	0.28 T

RESULTS AND DISCUSSION

All powering tests and measurements were performed at 77 K, in liquid nitrogen. The first current ramps were used to investigate the coil's behavior up to the region of the expected critical current I_c. Next, we investigated the voltage decay, thus the charging of the coils by applying current step functions. Finally, we tested the limits of our NI design and went with current steps well above the critical current and measured the radial resistance R_R.

The measured critical current of each sub-coil was derived from U-I measurements following an electric field criterion of 1 µV/cm and the length of the outermost turn (~30 cm). This assumption gives us a threshold value of 30 µV. The I_c of one VR coil is defined by min($I_{c,sub\text{-}coil1}$, $I_{c,sub\text{-}coil2}$). The Hall probe output has an accuracy of ±2%.

Current Ramps

Figure 3 shows exemplarily the measured voltage for each sub-coil of a VR coil when ramping the current with a ramp rate of 0.5 A/s up to plateaus of 10 A, 20 A, 30 A and 35 A. The VR coil's asymmetry lets us expect a different critical current per sub-coil due to the magnetic flux distribution in the superconductor [12]. With increasing current, the voltage is also expected to rise: most of the current will first penetrate the NI coil radially before settling into the superconducting path, which can then be detected as voltage decay. When the I_c of the superconductor is reached locally, the current is forced to flow radially and/or in the copper matrix of the coated super-conductor, which can be measured as an elevated asymptotic voltage plateau level after a decay time. As described above, the sub-coil's I_c is reached, once this constant voltage hits 30 µV. Similar voltage responses were found for all three VR coils.

Current Steps and Overflow

All three VR coils were powered gradually up to 112 A with a current step function of 2 A, followed by 300 s decay time before the next step. The decayed voltage and the Hall

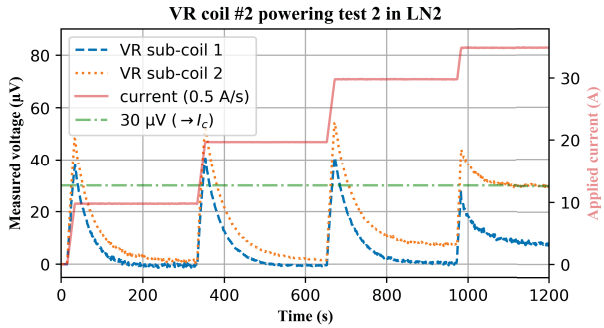

Figure 3: Voltage responses of each sub-coil for VR coil #2 caused by current ramps with 0.5 A/s ramping speed.

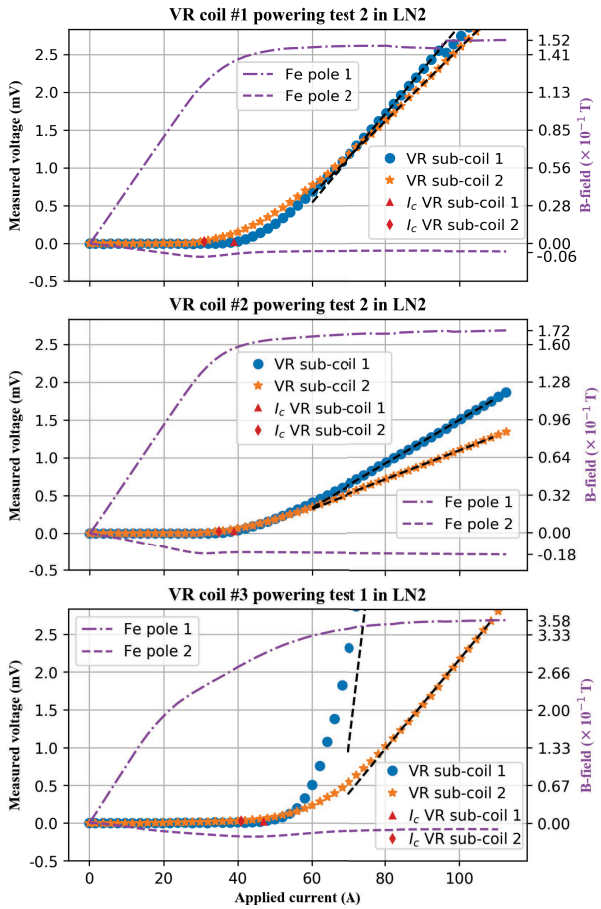

Figure 4: Measured voltages and magnetic pole fields of VR coil #1 (top), VR coil #2 (center) and VR coil #3 (bottom) for a current step function: 2 A step, 300 s hold. Black dashed lines represent linear fits of the radial resistance.

Table 2: Measured Parameters of the VR Undulator Coils

	VR coil #1		**VR coil #2**		**VR coil #3**	
Sub-coil	**1**	**2**	**1**	**2**	**1**	**2**
I_c (A)	40	30	39	35	47	41
$B_0(I_{c,sim})$ (cT)	1.29	0.16	1.35	0.18	2.75	0.24
R_R (µΩ)	58	48	29	19	400	58
τ (s)	26	42	32	46	(4)	90

ISBN: 978-3-95450-227-1 ISSN: 2673-5490 doi:10.18429/JACoW-IPAC2022-THPOPT058

probes' signal are shown in Fig. 4 for the tested VR coils. Measured values are displayed in Table 2.

VR coils #1 and #2 performed qualitatively as expected. The magnetic field B_0 increased up to I_c and reached the region of our predicted values for 30 A (6% and 2% disparity, respectively). After having reached I_c, B_0 began to stabilize and the sub-coils became increasingly resistive. With every current step more turns reached their local I_c and the V-I curve converges to Ohm's law, representing the radial resistance R_R across each sub-coil. Differences between the values within a VR coil can be seen as irregularities in the winding process. The difference between VR coil #1 and #2 can be explained by different winding tensions (30 N vs. 25 N) during manufacturing, which influences the contact resistance between tapes.

Sub-coil 2 in VR coil #3 performed as expected and described above, whereas sub-coil 1 showed a strong R_R. Yet, the region of calculated B_0 could be reached for 40 A with a disparity of 2%. Twice the number of turns let us expect a higher R_R compared to the previous coils. However, one order of magnitude discrepancy together with the non-saturated B_0 behavior for Fe pole 1 might indicate potential damage to the superconductor, which needs to be further investigated.

Effective Time Constants

When varying the undulator field for tuning to different photon energies of users' demands, it is crucial to know how fast an undulator can be charged or discharged. This can be indicated by the effective time constant τ, when measuring the above-mentioned voltage decay time after a current step, thus the time the current needs to enter or exit the superconducting path. The voltage decay can be approximated as exponential decay [15], [16]: $U \approx a \cdot e^{-t/\tau}$, with $\tau = L/R$, inductance L and constant a.

For all three VR coils, a current step to a plateau of 10 A for 300 s was applied, followed by a step to a plateau of 0.5 A for another 300 s, etc. The measured voltage is shown in Figure 5. VR coils #1 and #2 showed similar, expected behaviors: an exponential decay with similar τ_i for sub-coil 1 and 2, respectively, as noted in Table 2. Sub-coil 2 in VR coil #3 performed as described above. Twice the number of turns leads to a longer (dis-)charging time, here roughly doubles it.

As noticed before, VR coil #3's sub-coil 1 behaves differently. In the VR coil's series circuit, both sub-coils influence each other's (dis-)charging response, especially when one operates differently (see Fig. 6). Caused by the noticed defects in sub-soil 1, its voltage decay time was drastically reduced. For this reason, the slower decaying voltage of sub-coil 2 pulled/pushed current out/in of the sub-coil 1, which can be detected as a change of sign in the voltage signal.

CONCLUSION

We powered three non-insulated VR undulator coils at 77 K, in liquid nitrogen, each consisting of two sub-coils.

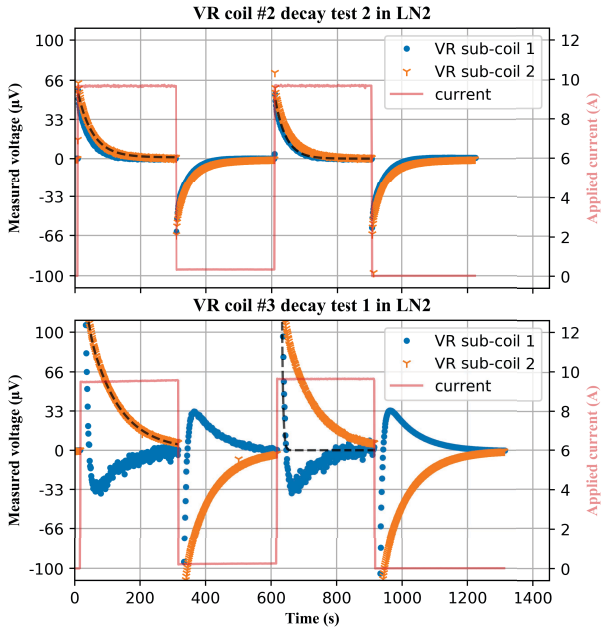

Figure 5: Measured decaying voltages of VR coil #2 (top), which also represents VR coil #1, and VR coil #3 (bottom). Black dashed lines represent exponential fits of the decay.

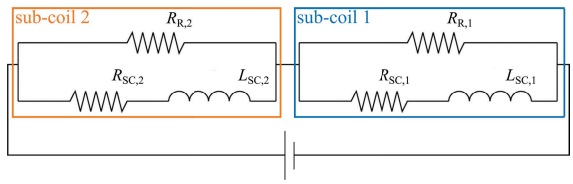

Figure 6: Simplified circuit diagram of one NI VR coil. Inside each sub-coil, the current can select between the radial resistive path $R_{R,i}$ and the superconducting, inductive path $R_{sc,i}$. Both sub-coil's inductances may interact.

All performances reached their design current of 30 A and 40 A with a magnetic peak field in the gap of 0.135 T and 0.275 T, respectively. This was verified in multiple electrical and thermal cycles. Moreover, all coils showed stable performances, even for currents beyond the critical current (~300% I_c), without any superconductor degradation. Measured time constants around 45 s for two of our three coils may be suitable for tunable undulators.

Summarized, we successfully demonstrated the application of ReBCO coated superconductors to undulator coils with $\lambda_u = 13$ mm and showed the stability and magnetic field performance of a non-insulated undulator coil design.

Next, we plan to power our HTS VR undulator coils at 4.2 K to investigate operations at high current densities (~2.3 kA/mm^2) and to explore the magnetic field limits.

ACKNOWLEDGMENTS

The authors would like to acknowledge C. Fernandes, J. Mazet, F. Garnier, F.-O. Pincot, P.-A. Contat, N. Bourcey, S. Clement, P. Martin Vazquez and J. C. Perez for support in the manufacturing process. G. Lenoir, P. Koziol and C. Barth are thanked for supporting the powering tests.

ISBN: 978-3-95450-227-1 ISSN: 2673-5490 doi:10.18429/JACoW-IPAC2022-THPOPT058

REFERENCES

[1] C. Boffo *et al.*, "Performance of SCU15: The New Conduction-Cooled Superconducting Undulator for ANKA", *IEEE Transactions on Applied Superconductivity*, vol. 26, no. 4, pp. 1-4, 2016. doi:10.1109/TASC.2016.2535861

[2] A. Bernhard *et al.*, "A CLIC Damping Wiggler Prototype at ANKA: Commissioning and Preparations for a Beam Dynamics Experimental Program", in *Proc. IPAC'16*, Busan, Korea, May 2016, pp. 2412–2415. doi:10.18429/JACoW-IPAC2016-WEPMW002

[3] Y. Ivanyushenkov *et al.*, "Development and operating experience of a short-period superconducting undulator at the advanced photon source", *Physical Review ST Accelerators and Beams*, vol. 18, no. 4, p. 040703, 2015. doi:10.1103/PhysRevSTAB.18.040703

[4] M. Tischer *et al.*, "Damping Wigglers for the Petra III Light Source", in *Proc. PAC'05*, Knoxville, TN, USA, May 2005, paper RPAE036, pp. 2446–2448. doi:10.1109/PAC.2005.1591140

[5] A. Bernhard *et al.*, "A CLIC Damping Wiggler Prototype at ANKA: Commissioning and Preparations for a Beam Dynamics Experimental Program", in *Proc. IPAC'16*, Busan, Korea, May 2016, pp. 2412–2415. doi:10.18429/JACoW-IPAC2016-WEPMW002

[6] S. C. Richter, "HTS undulator development", at the *CLIC Workshop 2019*, CERN, Geneva, January 2019, https://indico.cern.ch/event/753671/

[7] S. C. Richter *et al.*, "High-temperature superconducting undulators for compact free-electron lasers", in *Verhandlungen der Deutschen Physikalischen Gesellschaft, (Mueche2019issue)*, 1, March 2019.

[8] F. Nguyen *et al.*, "XLS - D5.1: Technologies for the Compact Light Undulator", on *Zenedo*, 2019. doi:10.5281/zenodo.5024409

[9] A. Golovashkin *et al.*, "Low temperature direct measurements of Hc2 in HTSC using megagauss magnetic fields", *Physica C: Superconductivity*, vol. 185-159, pp. 1859-1860, 1991. doi:10.1016/0921-4534(91)91055-9

[10] I. Kesgin, M. Kasa, Y. Ivanyushenkov, U. Welp, "High-temperature superconducting undulator magnets", *Superconductor Science and Technology*, vol. 30, no. 4, p. 04LT01, 2017. doi:10.1088/1361-6668/aa5d48

[11] Opera 2020, Simulation Software [online]. Available: https://www.3ds.com/de/produkte-und-services/simulia/produkte/opera/, 2020.

[12] J. Fleiter and A. Ballarino, "Parameterization of the critical surface of REBCO conductors from Fujikura", in *Internal CERN Notes*, 2014.

[13] M. Danial and J. van Nugteren, "Parameterization of the critical surface of REBCO conductors from Bruker", in *Internal CERN Notes*, 2017.

[14] CompactLight project (XLS) [online], Available: http://www.compact-light.eu/, Accessed April 2022.

[15] S. C. Richter *et al.*, "Progress on HTS Undulator Prototype Coils for Compact FEL Designs", *IEEE Transactions on Applied Superconductivity*, vol. 32, no. 4, pp. 1-5, June 2022. doi:10.1109/TASC.2022.3150288

[16] T. H. Nes *et al.*, "Effective Time Constants at 4.2 to 70 K in ReBCO Pancake Coils With Different Inter-Turn Resistances", *IEEE Transactions on Applied Superconductivity*, vol. 32, no. 4, pp. 1-6, June 2022. doi:10.1109/TASC.2022.3148968